# The role of tides in beach cusp development

Giovanni Coco,[1] Tom K. Burnet, and B. T. Werner

Complex Systems Laboratory, Cecil and Ida Green Institute of Geophysics and Planetary Physics, University of California, San Diego, La Jolla, California, USA

Steve Elgar

PVLAB, Woods Hole Oceanographic Institution, Woods Hole, Massachusetts, USA

[1] Field measurements of morphology and swash flow during three episodes of beach cusp development indicate that tides modulate the height and cross-shore position of beach cusps. During rising tide, beach cusp height decreases as embayments accrete more than horns and the cross-shore extent of beach cusps decreases. During falling tide, beach cusp height increases as embayments erode more than horns and cross-shore extent increases. A numerical model for beach cusp formation based on self-organization, extended to include the effects of morphological smoothing seaward of the swash front and infiltration into the beach, reproduces the observed spacing, position, and tidal modulation. During rising tide, water particles simulating swash infiltrate, preferentially in embayments, causing enhanced deposition. During falling tide, exfiltration of water particles combined with diversion of swash from horns causes enhanced erosion in embayments. Smoothing of beach morphology in the swash zone seaward of the swash front and in the shallow surf zone accounts for most of the observed tidal modulation, even in the absence of infiltration and exfiltration. Despite the qualitative, and in some cases quantitative, agreement of the model and measurements, the model fails to reproduce observed large deviations of horn orientation from shore normal, some aspects of beach cusp shape, and deviations from the basic tidal modulation, possibly because of the simplified parameterization of cross-shore sediment transport and the neglect of the effects of sea surface gradients on flow. *INDEX TERMS:* 4546 Oceanography: Physical: Nearshore processes; 4255 Oceanography: General: Numerical modeling; 3220 Mathematical Geophysics: Nonlinear dynamics; *KEYWORDS:* beach cusp, tides, infiltration, exfiltration, erosion

## 1. Introduction

[2] Beach cusps are swash zone morphological features with lunate bays and horns that protrude offshore, often forming a repeating pattern along the shoreline. Many studies of beach cusps have focused on the mechanisms underlying their initiation [*Guza and Inman*, 1975; *Dalrymple and Lanan*, 1976; *Dean and Maurmeyer*, 1980; *Inman and Guza*, 1982; *Werner and Fink*, 1993; *Masselink*, 1999; *Coco et al.*, 1999, 2001], whereas few studies have focused on the processes influencing the subsequent development and shape of beach cusps [*Williams*, 1973; *Dubois*, 1978; *Masselink and Pattiaratchi*, 1998; *Masselink et al.*, 1997; *Werner and Fink*, 1993; *Coco et al.*, 1999, 2003]. For example, the formation of beach cusps was related to the generation of a berm at low tide, with their cross-shore extent and the position of the berm observed to change with tide level [*Dubois*, 1978]. Permeability and infiltration rates that are larger at horns than at bays have been reported to result from grain size sorting, with coarser sediments at horns than at bays [*Longuet-Higgins and Parkin*, 1962; *Antia*, 1987]. Beach cusps result from both erosional [*Evans*, 1938; *Smith and Dolan*, 1960] and depositional [*Kuenen*, 1948; *Russell and McIntire*, 1965; *Takeda and Sunamura*, 1983] processes.

[3] Although beach cusps are common, their evolution from inception to well-developed forms responding to changing forcing conditions has not been carefully studied. Here numerical model simulations are compared with field observations for three distinct episodes of beach cusp formation and development. Beach cusp formation and evolution were observed to consist of a sequence of accretionary and erosional events related to both cuspate morphology and tidal stage. A numerical model based on self-organization [*Werner and Fink*, 1993; *Coco et al.*, 2000, 2003] was modified to include the effects of tidally dependent forcing conditions, morphological smoothing seaward of the swash front, and water infiltration, storage,

---

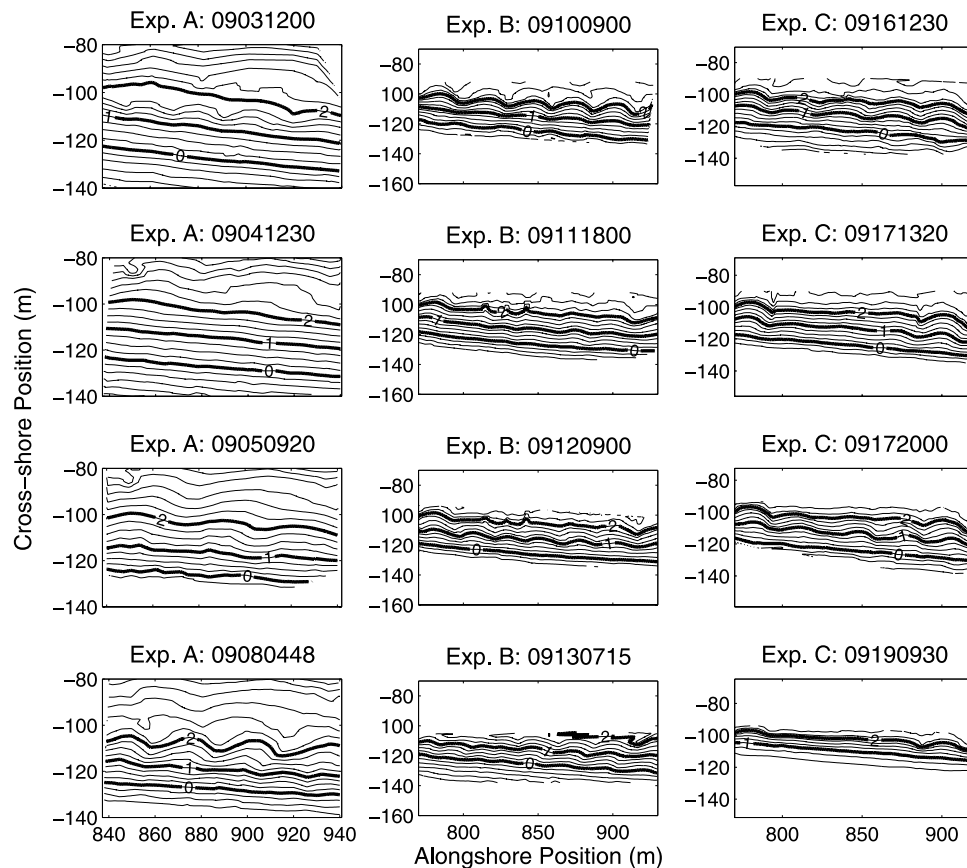[1]Now at National Institute of Water and Atmospheric Research, Hamilton, New Zealand.

**Figure 1.** Contours of beach bathymetry (elevation relative to mean sea level) as a function of cross-shore and alongshore position (scales differ for each experiment and seaward is down). (left) Beach cusps formed after a Nor'easter storm smoothed the beach in experiment A. Beach cusps re-formed after the beach was smoothed with a bulldozer in experiments (center) B and (right) C. A second Nor'easter storm smoothed the beach at the end of experiment C. Dates are in the form 'mmddhhhh' where mm is the month, dd the day, and hhhh the hour (EST) at the start of the survey. Bold curves are 0-, 1-, and 2-m elevation contours.

and exfiltration from a porous beach. Given measured forcing, model predictions for changing morphology are compared with measurements to assess the roles of tides, smoothing, and a porous beach on behavior of beach cusps.

## 2. Description of Field Experiments

[4] Three experiments were performed in September 1994 on a barrier island near Duck, North Carolina. The average foreshore slope was about 0.1 after extended periods of calm conditions and was lower during storms. The average sediment size was approximately 0.45 mm. The tide was semidiurnal with a 1-m range. Theodolite surveys were conducted to obtain morphology measurements and were performed at 3 to 4 hour intervals, with vertical uncertainty 0.03 to 0.05 m. Swash front motions were obtained from videotape images during daylight hours (for further details, see *Burnet* [1998] and *Coco et al.* [2003]). Beach cusp height, at a given elevation contour $z$, was measured as the difference between $z$ and the minimum elevation along a line spanning two beach cusp horns on the contour. In all three experiments, beach cusps formed after a section of beach with preexisting beach

cusps had been smoothed by either a storm or a bulldozer (Figure 1).

[5] In experiment A, beach cusp morphology was measured from noon of September 3 until the morning of September 8 (Figures 1 and 2). Beach cusps were smoothed by a storm between noon September 3 and noon September 4. During rising tide, the beach accreted near the 1-m depth contour, with bays accreting more than horns (Figures 2a, 09051200–09051939, and 2c, 09070400–09070600, where 09051200 signifies the survey starting on September 5 at 1200 EST). Near high tide, horns accreted near the 2-m contour and bays eroded near the 1-m contour. During falling tide, the beach eroded, with bays tending to erode more than horns accreted (Figures 2b, 09060921–09061200, and 2d, 09070945–09071220). During the experiment, horns projected first southward ($\approx+7°$ with respect to the mean beach normal, Figure 2a, 09051939), then northward ($\approx-9°$, Figure 2b, 09061200), and again southward ($\approx+6°$, not shown, 09080600). In the section of beach monitored, two horns migrated to the north (+5 m) while one horn migrated to the south ($-10$ m) as beach cusp spacing decreased from about 30 to 25 m (the change occurred between 09061835 and 09062210 and can be
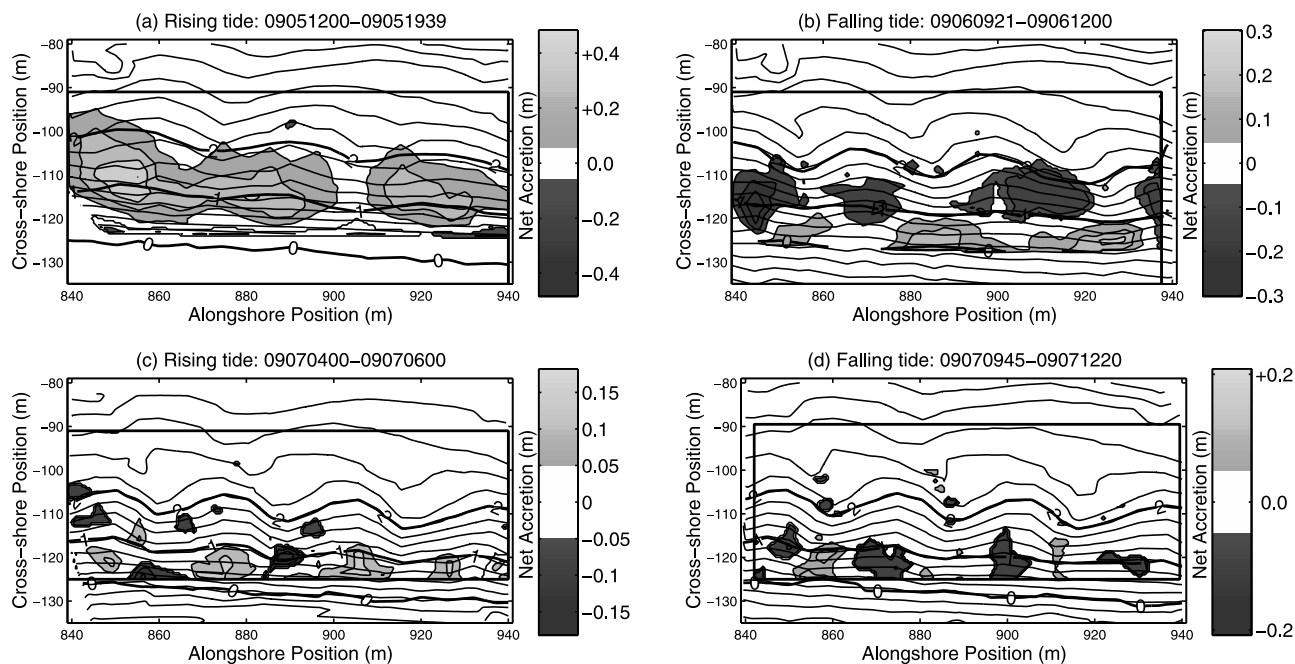
**Figure 2.** Contours of beach bathymetry (elevation relative to mean sea level) as a function of cross-shore and alongshore position during experiment A (seaward is down). The inner frame highlights the area where patterns in accretion and erosion have been evaluated. Light shading indicates accretion; dark shading indicates erosion; white indicates accretion or erosion less than 0.05 m. Maximum accretion and erosion are (a) 0.48 and −0.16 m (09051200–09051939), (b) 0.24 and −0.30 m (09060921–09061200), (c) 0.16 and −0.18 m (09070400–09070600), and (d) 0.21 and −0.11 m (09070945–09071220). Contours are from the later of the two surveys. Bold curves are 0-, 1-, and 2-m elevation contours.
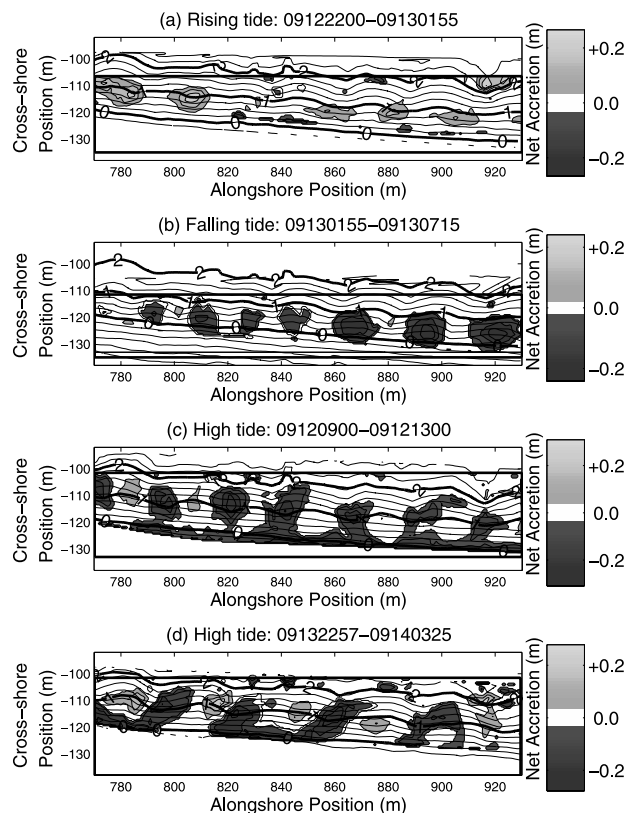


observed by comparing beach cusp spacing between surveys 09061200 and 09070600, Figures 2b and 2c).

[6] In experiment B, beach cusp morphology was measured from the morning of September 10 until the morning of September 14 (Figures 1 and 3). At the beginning of the experiment, deltas just offshore of bays were measured with heights up to 0.25 m relative to morphology offshore of horns (not shown). Beach cusps were smoothed by a bulldozer on the morning of September 11. During parts of the experiment, the beach responded similarly to that observed during experiment A, with accretion in bays during rising tide (Figure 3a, 09122000–09130155), accretion on horns and erosion in bays at high tide, and erosion in

**Figure 3.** Contours of beach bathymetry (elevation relative to mean sea level) as a function of cross-shore and alongshore position during experiment B (seaward is down). The inner frame highlights the area where patterns in accretion and erosion have been evaluated. Light shading indicates accretion; dark shading indicates erosion; white indicates accretion or erosion less than 0.05 m. Maximum accretion and erosion are (a) 0.26 and −0.11 m (09122200–09130155), (b) 0.18 and −0.31 m (09120900–09121300), (c) 0.10 and −0.24 m (09130155–09130715), and (d) 0.28 and −0.26 m (09132257–09140325). Contours are from the later of the two surveys. Bold curves are 0-, 1-, and 2-m elevation contours.
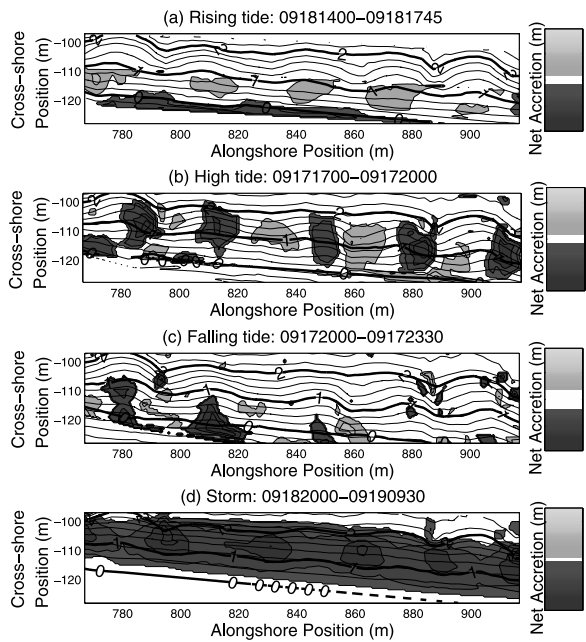
**Figure 4.** Contours of beach bathymetry (elevation relative to mean sea level) as a function of cross-shore and alongshore position during experiment C (seaward is down). Light shading indicates accretion; dark shading indicates erosion; white indicates accretion or erosion less than 0.05 m. Maximum accretion and erosion are (a) 0.39 and −0.20 m (09181400–09181745), (b) 0.13 and −0.19 m (09172000–09172330), (c) 0.23 and −0.28 m (09171700–09172000), and (d) 0.23 and −0.69 m (09182000–09190930). Contours are from the later of the two surveys. Bold curves are 0-, 1-, and 2-m elevation contours.

bays during falling tide (Figure 3b, 09130155–09130715). However, during two high tides, horns eroded as bays accreted (Figures 3c, 09120900–09121300, and 3d, 09132257–09140325). During one of these high tides (09120900–09121300), high-frequency wind waves incident from the north were observed. During the experiment, horns projected northward ($\approx -12°$, not shown, 09120100) and then southward ($\approx +5°$, Figure 3b, 09130715). Two horns migrated to the north and merged as the overall beach cusp spacing increased from about 25 to 30 m (the change occurred between 09131100 and 09131614 and can be observed by comparing beach cusp spacing between surveys 09121300 and 09140325, Figures 3c and 3d). Three small channels artificially created on the upper beach (alongshore position 810 to 850 m along the 2 m contour for 09111800 in Figure 1) did not affect formation of beach cusps and were filled slowly.

[7] In experiment C, beach cusp morphology was measured from noon of September 16 until noon of September 20 (Figures 1 and 4). Beach cusps were smoothed by a bulldozer on the morning of September 17. For two tidal cycles, the beach responded in a manner similar to that observed during experiment A, with accretion in bays during rising tide (Figure 4a, 09181400–09181745), accretion in horns and erosion in bays at high tide (Figure 4b, 09172000–09172000), and erosion in bays during falling tide (Figure 4c, 09172000–09172330). Then, storm waves
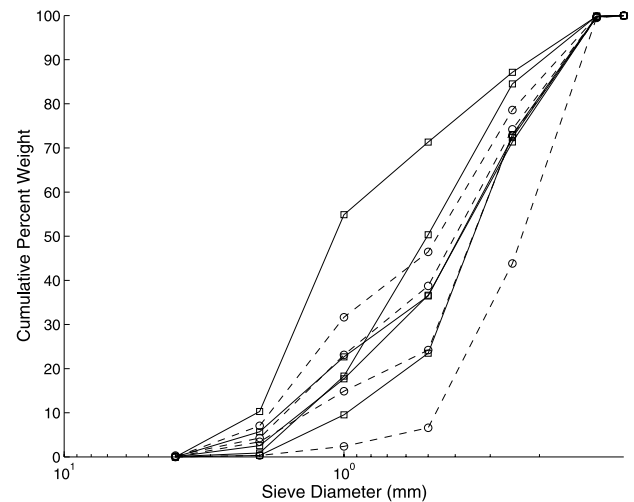


**Figure 5.** Cumulative percent weight of sediment in horns (squares) and bays (circles) versus sieve diameter.

eroded the beach and largely destroyed the beach cusps (Figure 4d, 09182000–09190930). During calmer wave conditions, the beach accreted, but beach cusps did not reform during the experiment. The horns projected northward ($\approx -11°$, Figure 4c, 09172300) and then slightly southward ($\approx +7°$, not shown, 09180800).

[8] Sediment grain size often is larger on horns than in bays [*Kuenen*, 1948; *Russell and McIntire*, 1965; *Williams*, 1973; *Chafetz and Kocurek*, 1981; *Antia*, 1987; *Masselink et al.*, 1997]. These differences in sediment size have been hypothesized to create alongshore variability in infiltration rates. In experiments A-C [*Burnet*, 1998] grain size ($d_{50}$) differences between horns and bays were less than 1 standard deviation (0.00025 m) in seven (nonadjacent) of nine samples (Figure 5), suggesting that alongshore variations in infiltration rates owing to differences in sediment size might be insignificant at this location.

[9] As beach cusps began to develop, the maximum increase in measured height occurred near the upper limit of the swash front. Beach cusps waxed and waned with the
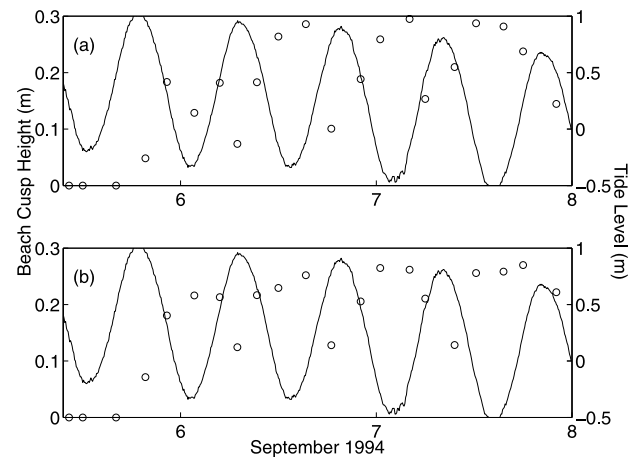


**Figure 6.** Beach cusp height (circles) as a function of time at elevation 1.2 m during experiment A for two horn-bay-horn systems centered at alongshore position (a) 870 m and (b) 900 m. The solid curve is tide level.

tide (Figure 6). Typically, beach cusps waned during rising tide because bays accreted more than horns, and waxed during falling tide and sometimes during the initial stages of the rising tide because bays eroded more than horns. However, during two rising tides, beach cusps waned because horns eroded more than bays. Horns also eroded during storms at the beginning of experiment A and at the end of experiment C. The cross-shore position of beach cusps also is modulated by tides, with beach cusps extending farther offshore during falling tide and contracting onshore during rising tide (Figures 7 and 8). The magnitudes of the changes in the beach cusp cross-shore extent are similar to variations in tidal elevation, so that a spring-neap trend is observed.

## 3. Model Description

[10] Motion of the swash front is simulated using independent water particles that, for each swash cycle, are given an initial velocity up the beach and then move under gravity on the beach surface [*Coco et al.*, 2000]. Initial water particle velocity is chosen from a distribution that is independent of alongshore position and derived from measured 2-hour time series of swash front position (described by *Coco et al.* [2003]). The assumption that the initial velocity of the swash front up the beach is independent of beach cusp morphology might be violated if rundown interacts with incoming bores or if bores collapse into swash onshore of the position where significant beach cusp morphology is found. During the night, when swash measurements were not available, the closest swash times series was used, with the mean elevation being corrected for tidal variation using a pressure sensor deployed in shallow water.

[11] The model was initialized with observed morphology [*Coco et al.*, 2003]. Erosion and deposition of sediment results from changes in the carrying capacity of water particles, which is assumed to vary as the square of the water particle velocity so that sediment fluxes [*Werner and Fink*, 1993] are given by

$$Q(x,y,t) = \alpha u^3(x,y,t). \tag{1}$$

**Figure 8.** Minimum beach elevation at which beach cusps can be detected (circles) as a function of time during experiment A for two horn-bay-horn systems centered at alongshore position (a) 870 m and (b) 900 m. The solid curve is tide level.

The constant $\alpha$ is set to 0.008 s$^2$/m [*Coco et al.*, 2000, 2003] and $u$ is the water particle velocity at cross-shore position $x$, alongshore position $y$, and time $t$. Local smoothing of morphology is performed at the position of water particles and the surrounding five cell by five cell area (corresponding to 2.5 × 2.5 m) to minimize local variation from a plane.

[12] The model was extended to account for two processes that could underlie the observed tidal modulation of beach cusp height and extent (section 2). First, cuspate morphology developed at low tide levels in the thin flow near the swash front can be smoothed by deeper flow in the deep swash and shallow surf zones at high tide. This smoothing occurs because pressure gradients induced by bottom morphology, necessary for feedbacks leading to self-organized beach cusp formation, can be overwhelmed by sea-surface pressure gradients. Resultant tidal modulations of beach cusp height measured at a specific elevation are minimum during falling tide when the base of the thin swash tongue moves below that elevation. During rising tide, beach cusp height is maximum just before the base of the thin swash tongue moves above the elevation at which beach cusp height is measured.
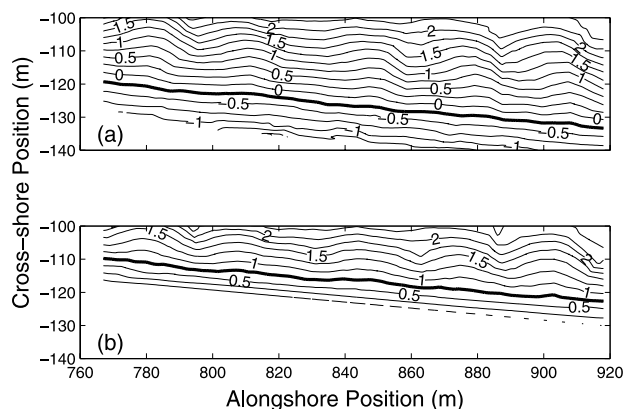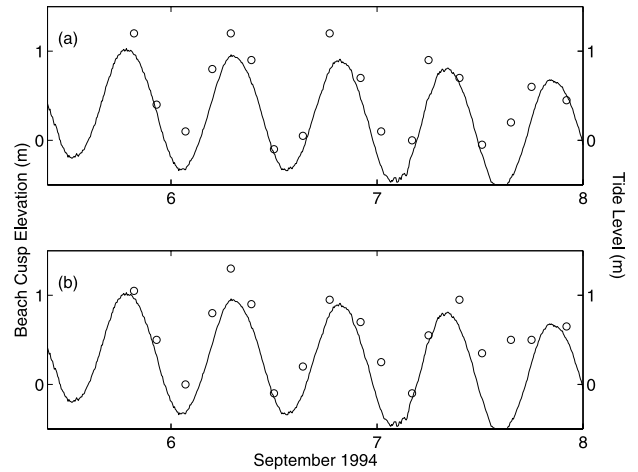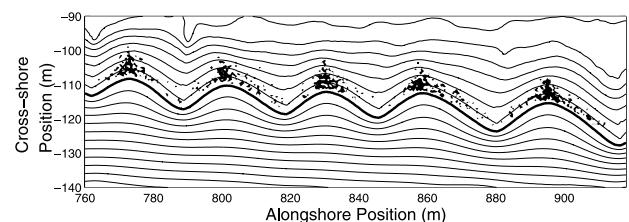
**Figure 7.** Contours of bathymetry (elevation relative to mean sea level) as a function of cross- and alongshore position during experiment C at (a) low tide (09172330) and (b) high tide (09182000). The bold curve separates cuspate from planar morphology.

**Figure 9.** Contours of bathymetry as a function of cross-shore and alongshore position. Each dot represents a water particle that infiltrated over a 2-hour period. Simulated water particles predominantly infiltrate in bays above the seepage front (bold curve).
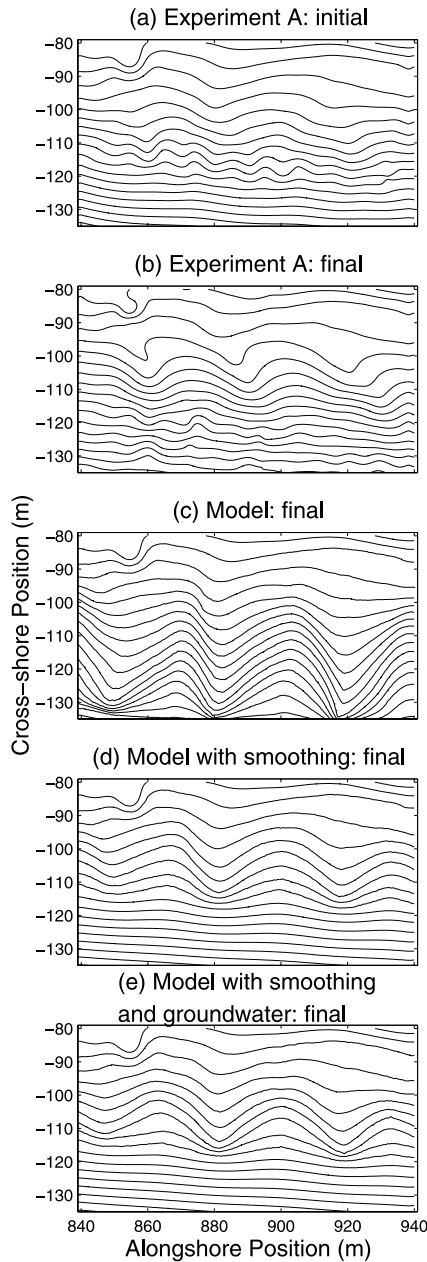
**Figure 10.** Contours of bathymetry as a function of cross-shore and alongshore position for experiment A. (a) Initial (09060445) and (b) final (09061525) surveyed morphology. Numerical simulation of beach cusp development from 09060445 to 09061525 initialized with morphology in Figure 10a and measurements of swash flow for (c) unmodified model, (d) model modified to include smoothing, and (e) model modified to include both smoothing and groundwater effects.

[13]　Smoothing is simulated by adding a linear diffusion term to the sediment flux [*Schielen et al.*, 1993; *Falqués et al.*, 1996, 2000],

$$Q(x,y,t) = \alpha u(x,y,t)^3 - \gamma \nabla(h - h_0), \qquad (2)$$

where $\gamma$ is a morphological diffusion constant (taken to be 0.75 m²/s), $h$ is the elevation of the beach, and $h_o$ is a

reference surface, defined here as the alongshore average surface of the beach at the start of each simulation.

[14]　Second, water in swash can infiltrate into a beach when the swash front rises above the groundwater table, usually during rising tide [*McArdle and McLachan*, 1991; *Turner and Masselink*, 1998]. Similarly, water can exfiltrate from a porous beach where the groundwater table outcrops above the swash [*Grant*, 1948; *Duncan*, 1964]. The groundwater table can lag significantly behind the mean water level for a broad range of hydraulic conductivities typical of beach sands [*Emery and Foster*, 1948; *Duncan*, 1964; *Nielsen*, 1990; *Turner*, 1995]. Percolation through the porous beach can lead to tidal modulation of erosion and deposition, because, during rising tide, infiltration leads to net accretion whereas, during falling tide, exfiltration causes net erosion [*Grant*, 1948; *Duncan*, 1964]. On a cuspate beach, the diversion of swash from horns to bays leads to an alongshore variation in tidal modulation. In contrast to the effects of morphological smoothing, during rising tide, bays accrete more than horns and beach cusps wane so that beach cusp height is minimum as the groundwater table rises above the elevation at which beach cusp height is measured. During falling tide, bays erode more than horns and beach cusps wax so that beach cusp height is maximum as the groundwater table passes through the elevation at which beach cusp height is measured.

[15]　In the model, infiltration of water particles above the groundwater table is simulated by their elimination with probability $P$ (whereupon they drop their sediment load). In accordance with measurements collected on a cuspate beach for more than one tidal cycle (≈40 hours with vertical swash excursion = 1.75 m, $d_{50}$ = 0.00035 m, hydraulic conductivity ≈0.0007 m/s, and beach slope = 0.12 [*Eliot and Clarke*, 1986]), and assuming negligible alongshore differences in set-up, the groundwater table is assumed to be elevated 1 m above the lower swash limit during rising tide. These values are comparable to values measured at this field site: $d_{50}$ = 0.0005 m, hydraulic conductivity ≈0.001 m/s [*Turner and Masselink*, 1998], mean vertical swash excursion = 1.15 m, and mean beach slope = 0.06
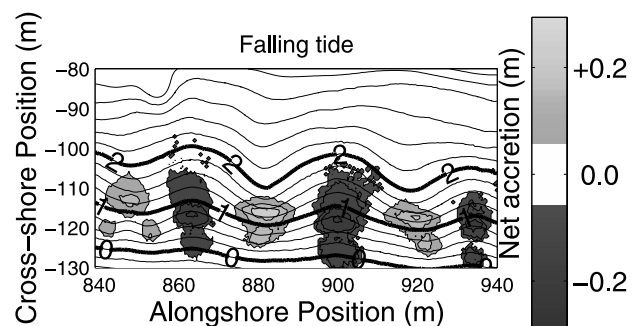


**Figure 11.** Contours of bathymetry (elevation relative to mean sea level) as a function of cross-shore and alongshore position for model simulation with smoothing and groundwater effects (experiment A). Light shading indicates accretion; dark shading indicates erosion; white indicates accretion or erosion less than 0.05 m. Maximum accretion and erosion are 0.29 and −0.25 m (falling tide, corresponding to approximately 09060921–09061200). Bold curves are 0-, 1-, and 2-m elevation contours.
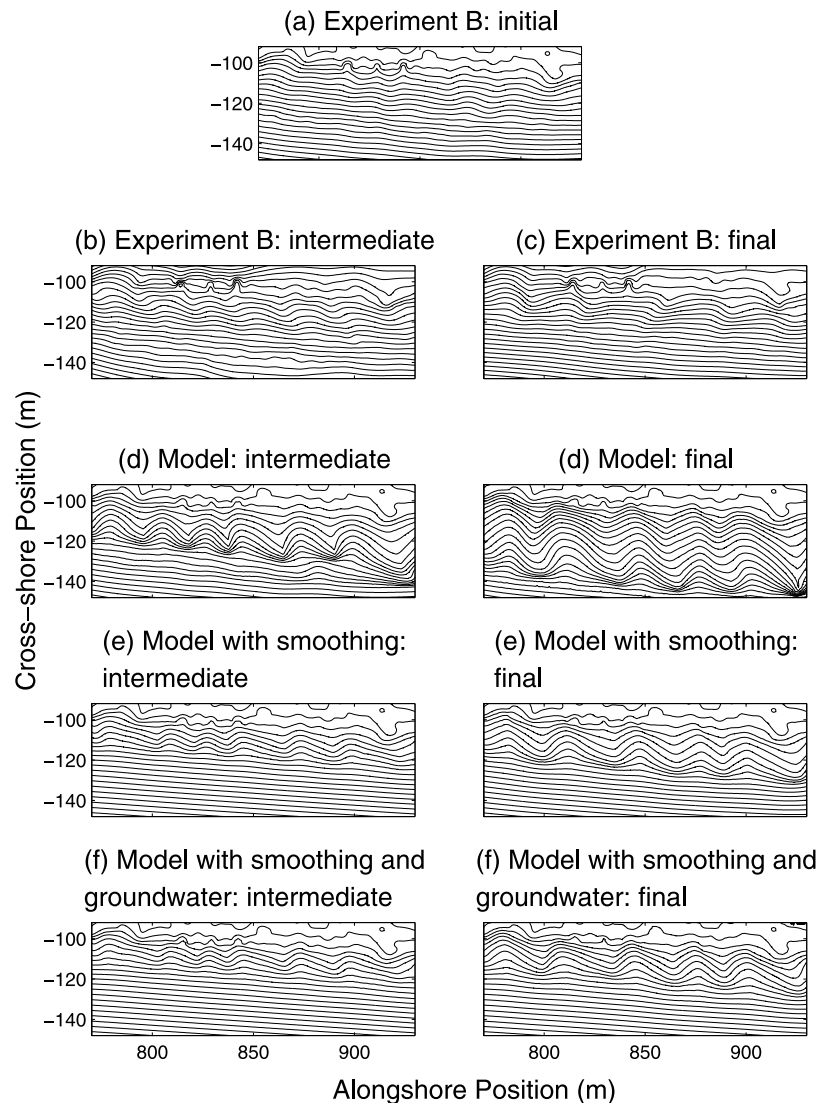
(a) Experiment B: initial

(b) Experiment B: intermediate          (c) Experiment B: final

(d) Model: intermediate          (d) Model: final

(e) Model with smoothing:          (e) Model with smoothing:
intermediate          final

(f) Model with smoothing and          (f) Model with smoothing and
groundwater: intermediate          groundwater: final

Cross-shore Position (m)

Alongshore Position (m)

**Figure 12.** Contours of bathymetry as a function of cross-shore and alongshore position for experiment B. (a) Initial (09111800), (b) 11-hour (09120500), and (c) final (09131925) surveyed morphology. Numerical simulation of beach cusp development from 09111800 to 09131925 initialized with morphology in Figure 12a and measurements of swash flow for (d) unmodified model, (e) model modified to include smoothing, and (f) model modified to include both smoothing and groundwater effects.

(during experiment A: 09060445). Modeled infiltration and consequent deposition are concentrated in bays because of convergence of flow owing to cuspate morphology (Figure 9). Water particles that infiltrate are stored and distributed evenly along the beach as the spreading of groundwater horizontally between bays and cusps separated by 12 m occurs in 1.5 hours, somewhat faster than the 2 hours over which the characteristics of the swash are measured and averaged.

[16] Exfiltration is simulated by release of stored water particles when the elevation of the groundwater table exceeds the mean elevation of the swash front (calculated over the 2-hour videotape time series). The probability of stored water particle release is set to be proportional to the length of the seepage face, the cross-shore distance between where the groundwater table outcrops, and the

mean position of the swash front. The proportionality constant is chosen so that all water particles that infiltrate during rising tide exfiltrate during falling tide (on average). Exfiltrated water particles are released with zero velocity and no sediment. In accordance with measurements [*Turner*, 1995], the vertical velocity with which the groundwater table descends during falling tide, $V_s$, is set to

$$V_s = \frac{K \sin^2 \beta}{n}, \qquad (3)$$

where $K$ is hydraulic conductivity, $n$ is porosity, and $\beta$ is beach slope.

[17] Estimates of hydraulic conductivity vary by as much as an order of magnitude [*Butt et al.*, 2001; *Masselink and*
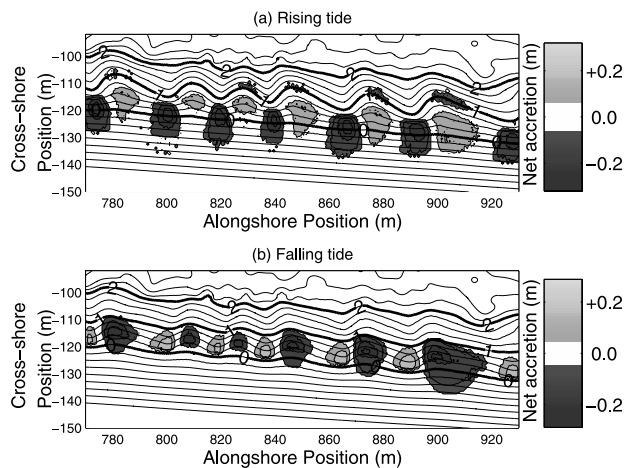
**Figure 13.** Contours of bathymetry (elevation relative to mean sea level) as a function of cross- and alongshore position for model simulation with smoothing and groundwater effects (experiment B). Light shading indicates accretion; dark shading indicates erosion; white indicates accretion or erosion less than 0.05 m. Maximum accretion and erosion are 0.24 and −0.32 m ((a) rising tide, corresponding to approximately 09120600–09120800), 0.19 and −0.28 m ((b) falling tide, corresponding to approximately 09130155–09130355). Bold curves are 0-, 1-, and 2-m elevation contours.

*Li*, 2001], but with $n \simeq 0.45$ and grain size $\simeq 0.0005$ m, a typical value [*Bear*, 1972; *Turner and Masselink*, 1998] is $K \simeq 0.001$ m/s. Hydraulic conductivity is related to probability of infiltration $P$ by assuming a constant swash zone depth $dh$ of 0.10 m. The time required for such a layer of water to infiltrate is $dh/K$, and therefore the probability of infiltration $P$ in a time step $dt$ is $dt * K/dh$. Boundary layer effects and vertical fluid drag have been linked to infiltration and exfiltration processes [*Butt et al.*, 2001], but their role, over timescales simulated in this study, is limited.

## 4. Model-Data Comparisons

[18] Numerical simulations conducted with a single set of parameters employing both the effects of groundwater and morphological smoothing seaward of the swash front reproduce the observed development, size, location, and tidal modulation of beach cusps, but some details, including beach cusp shape and the orientation of horns, often are not reproduced. The model was run without smoothing and groundwater effects, with just smoothing, and with both smoothing and groundwater effects.

[19] In experiment A, owing to limited measurements of swash and morphology, numerical simulations were restricted to 100 m alongshore and an 11-hour time period (09060445 to 09061525), over which beach cusps grew and their horns changed orientation (Figures 10a and 10b). The model reproduces the development, size, and location of beach cusps (Figures 10c–10e). Inclusion of smoothing results in beach cusps with the approximate observed cross-shore extent (Figure 10d). The effect of infiltration on the final beach cusp configuration is negligible (Figure 10e). Although the restricted time period precluded a full test of the observed

tidal modulation, numerical simulations with smoothing, and with smoothing and groundwater effects show deposition on horns and erosion in bays during falling tide, a pattern similar to measurements (compare Figure 11 with Figure 2b). The model failed to reproduce the northward orientation of beach cusps observed on 6 September (Figure 2b).

[20] Measured morphology from experiment B was compared with model results on a 150-m alongshore stretch of beach for a 50-hour time period (09111800 to 09131925), during which beach cusps formed from an approximately planar beach and increased in spacing, while horn orientation changed. All three versions of the model reproduce beach cusp location, spacing, and spacing increase through merger of the beach cusps located between 800 and 850 m (Figure 12). After 11 hours, models with smoothing simulate the observed offshore extent of beach cusps, but after 50 hours, modeled horns project slightly offshore from measured horns (Figure 12). All versions of the model
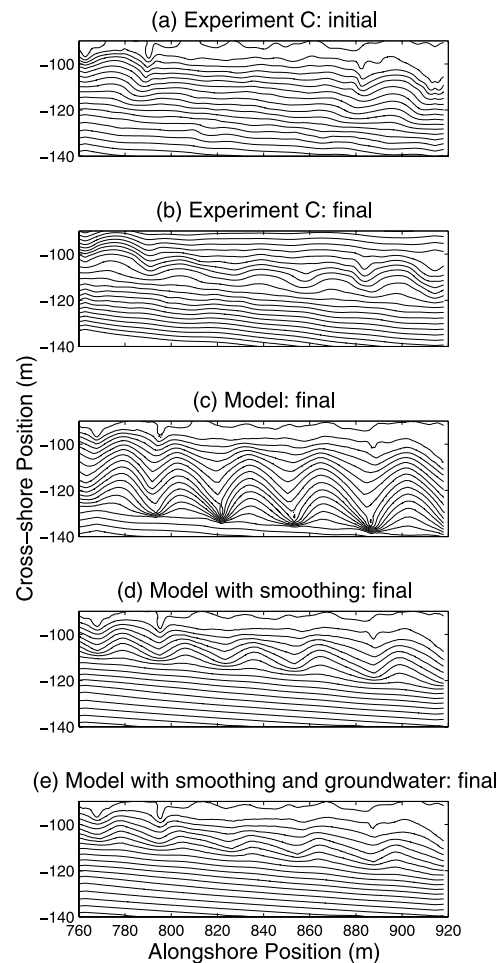


**Figure 14.** Contours of bathymetry as a function of cross-shore and alongshore position for experiment C. (a) Initial (09171320) and (b) final (09181745) surveyed morphology. Numerical simulation of beach cusp development from 09171320 to 09181745 initialized with morphology in Figure 14a and measurements of swash flow for (c) unmodified model, (d) model modified to include smoothing, and (e) model modified to include both smoothing and groundwater effects.
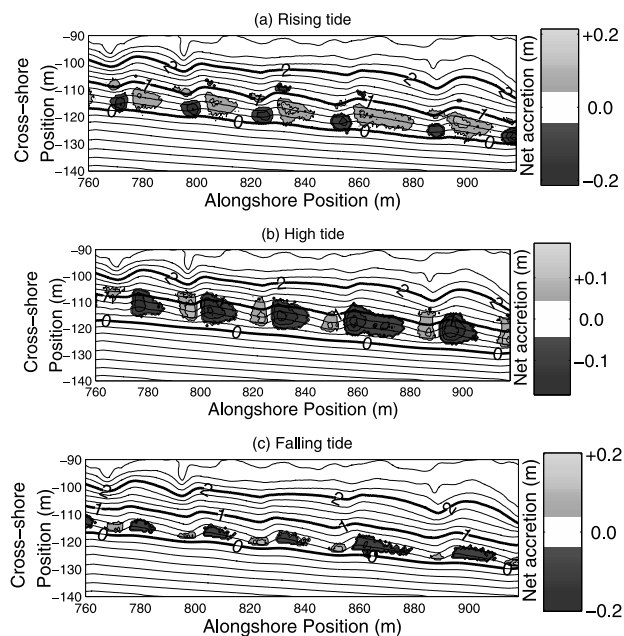
**Figure 15.** Contours of bathymetry (elevation relative to mean sea level) as a function of cross-shore and alongshore position for model simulation with smoothing and groundwater effects (experiment C). Light shading indicates accretion; dark shading indicates erosion; white indicates accretion or erosion less than 0.05 m. Maximum accretion and erosion are 0.14 and −0.21 m ((a) rising tide, corresponding to approximately 09180400–09180600), 0.15 and −0.18 m ((b) high tide, corresponding to approximately 09171700–09172000), 0.20 and −0.12 m ((c) falling tide, corresponding to approximately 09172000–09172330). Bold curves are 0-, 1-, and 2-m elevation contours.



**Figure 16.** Beach cusp height as a function of time at elevation 0.8 m. Symbols are observations (stars) and numerical simulations with smoothing (squares) and smoothing and groundwater effects (circles) of experiment C for two horn-bay-horn systems centered at alongshore position (a) 780 m and (b) 840 m. The curve is tide level. Model runs were initialized with morphology from experiment C (09171320 and Figure 14a) and run for 28 hours.

not modeled well. Smoothing and groundwater effects improve the shape by reducing the aspect ratio, but the modeled bays are steeper than measured bays. As with the other experiments, the general pattern of tidal modulation of beach cusps is reproduced with the model (compare Figure 15 with Figure 4).

[22] For all three experiments, modeled beach cusps waxed and waned (Figure 16), and changed their cross-shore position (Figure 17) with changing tidal level in a



**Figure 17.** Minimum beach elevation at which beach cusps can be detected as a function of time. Symbols are observations (stars) and numerical simulations with smoothing (squares) and numerical simulation with smoothing and groundwater effects (circles) of experiment C for two horn-bay-horn systems centered at alongshore position (a) 780 m and (b) 840 m. The curve is tide level. Model runs were initialized with morphology from experiment C (09171320 and Figure 14a) and run for 28 hours.

exhibit significant morphological change at least 5 m onshore of the upper limit of measured change on the beach, resulting in modeled infilling of the artificial channels, which changed only slightly on the natural beach. The models with smoothing exhibit the observed pattern of changes in orientation of horns, but with orientation that differed from those measured. Although the general pattern of tidal modulation appears in the model with smoothing and in the model with smoothing and groundwater effects (Figure 13), the observed erosion on horns and accretion in bays at high tide (Figure 3) are not reproduced with the model.

[21] Numerical simulations over 160 m alongshore and 28 hours (09171320 to 09181745) for experiment C, during which beach cusps formed and underwent slight changes in orientation, reproduce the measured spacing and positions of beach cusps (Figure 14). The models with smoothing (Figures 14d and 14e) correctly predict the offshore extent of horns (Figure 14b), but the onshore extent of beach cusps is overpredicted by approximately 5 m with smoothing only (Figure 14d). This overprediction is remedied partially with the inclusion of groundwater effects, because infiltration causes a reduction in the number of water particles reaching the upper beach. The shape of beach cusps in experiment C, characterized by high aspect ratio (spacing to cross-shore extent) and flat-bottomed bays, is
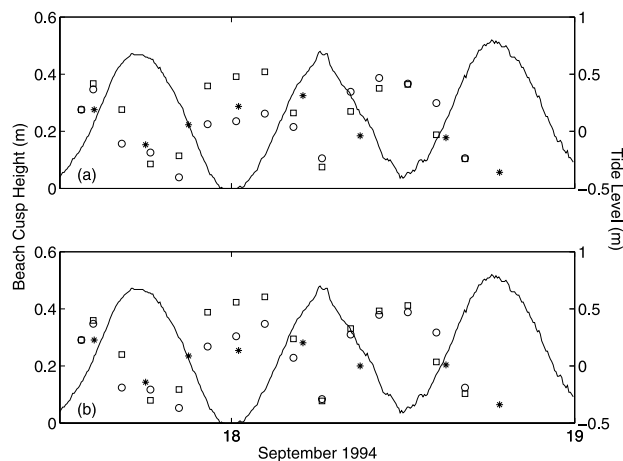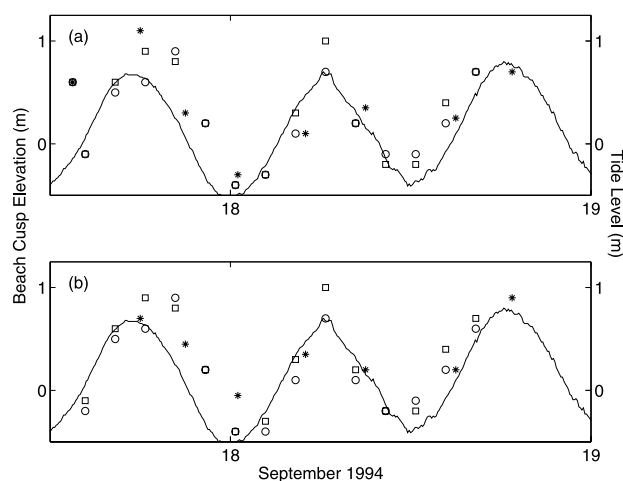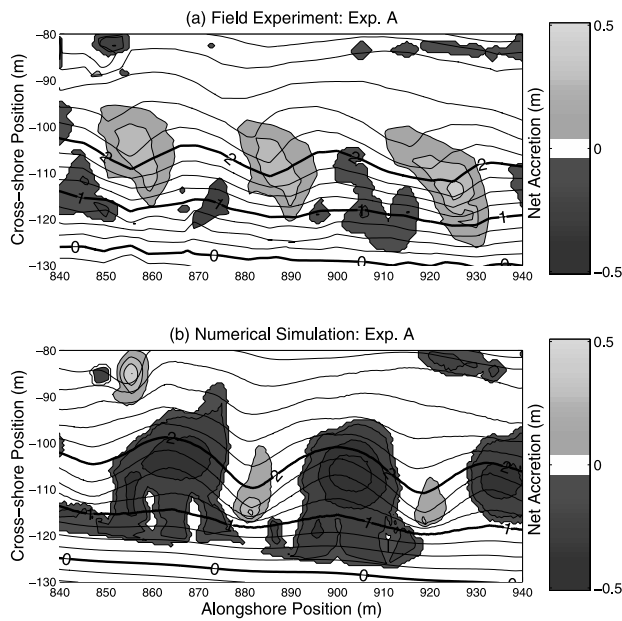
**Figure 18.** Contours of bathymetry (elevation relative to mean sea level) as a function of cross- and alongshore position for experiment A. (a) Observed net morphological change, and (b) modeled (smoothing and groundwater effects) net morphological change. Light shading indicates accretion; dark shading indicates erosion; white indicates accretion or erosion less than 0.05 m. Contour lines are taken from the later of the two surveys. Bold curves are 0-, 1-, and 2-m elevation contours. The model reproduces the patterns of erosion and deposition well, but overall magnitudes and changes associated with beach cusp reorientation and migration and with cross-shore sediment transport are not reproduced in detail.

manner similar to field observations (Figure 6). Simulations with groundwater effects usually result in a smaller reduction in beach cusp relief, and in some instances can be closer to observations than simulations without groundwater effects. However, significant deviations between modeled and measured modulations in beach cusp height were found during some tidal cycles. Direct measurement of swash forcing was available only during daylight; differences between model results and observations could have resulted from changes in swash excursion and incident wave angle during nighttime that are not included in model simulations.

[23] Comparisons of modeled with measured net morphological changes illustrate limitations of the model with respect to sediment transport and beach cusp orientation. The general pattern of erosion and deposition observed in experiment A is reproduced by the model (Figure 18), but the model fails to reproduce the morphological change associated with reorientation and migration of beach cusps. Significant net erosion occurred in the lower regions of the swash zone during experiment B, with deposition on horns limited to the upper swash zone (Figure 19a). In contrast, the pattern of erosion in bays and deposition on horns extends throughout the modeled swash zone (Figure 19b). In experiment C (Figures 19c and 19d), the primary difference between the patterns of erosion and deposition can be attributed to large measured changes in the orienta-

tion of beach cusps, which were not reproduced in the model. The factor of 2 difference between modeled and observed morphological change may be the result of parameterizing sediment transport with simple formulas.

[24] Modeled morphology depends somewhat sensitively on hydraulic conductivity. As hydraulic conductivity is increased, beach cusp height is reduced, because an increasing number of water particles infiltrate, reducing the positive feedback associated with water particle diversion (Figure 20a). For hydraulic conductivity $K \geq 0.003$ m/s (Figure 20a), beach cusps do not form. Instead, a steep ridge develops where infiltration is focused, qualitatively consistent with previous calculations showing that higher values of hydraulic conductivity enhance onshore sediment transport in the swash zone and lead to the development of steeper cross-shore profiles [*Masselink and Li*, 2001]. Beach cusp
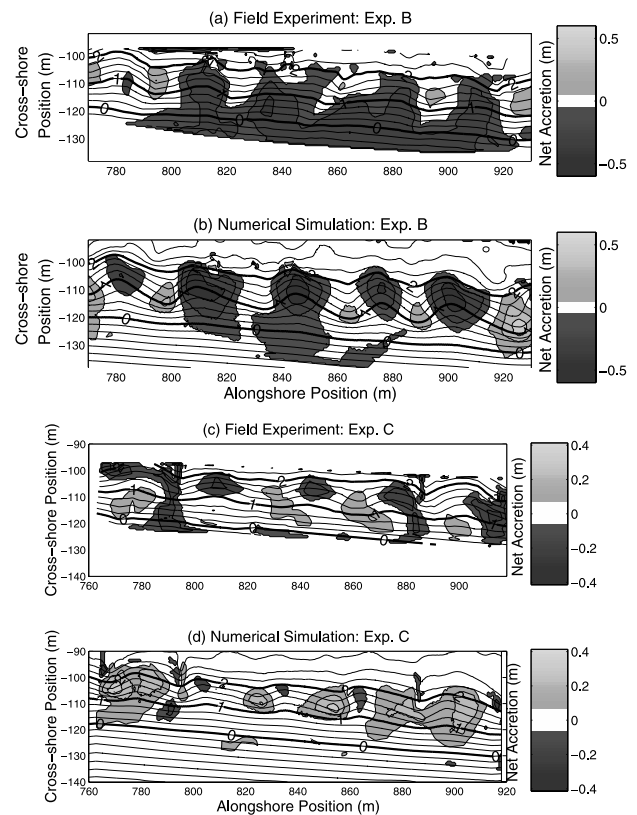


**Figure 19.** Contours of bathymetry (elevation relative to mean sea level) as a function of cross- and alongshore position. (a) Observed net morphological change for experiment B, (b) modeled (smoothing and groundwater effects) net morphological change for experiment B, (c) observed net morphological change for experiment C, and (d) modeled (smoothing and groundwater effects) net morphological change for experiment C. Light shading indicates accretion; dark shading indicates erosion; white indicates accretion or erosion less than 0.05 m. Contour lines are taken from the later of the two surveys. Bold curves are 0-, 1-, and 2-m elevation contours. The model reproduces the patterns of erosion and deposition well, but overall magnitudes and changes associated with beach cusp reorientation and migration and with cross-shore sediment transport are not reproduced in detail.
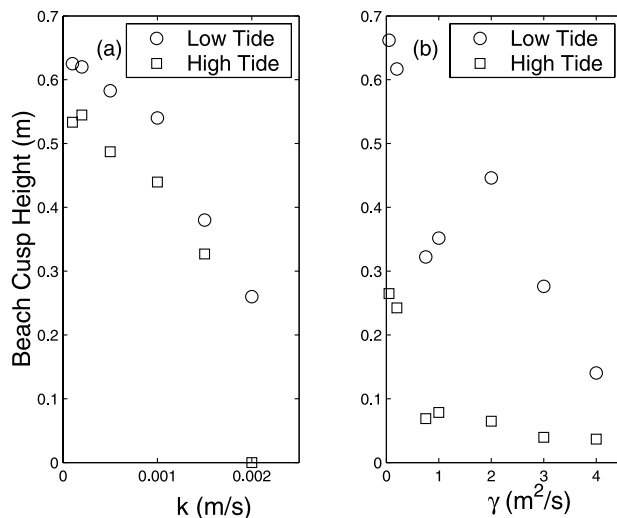
**Figure 20.** Beach cusp height versus (a) morphodynamic diffusion $\gamma$ (for $K = 0.0002$ m/s) and (b) hydraulic conductivity $K$ (for $\gamma = 0.05$ m²/s). Model runs were initialized with morphology from experiment C (09171320 and Figure 14a) and run for 16 hours at high tide (squares) and for 22 hours at low tide (circles).

formation also is suppressed as morphodynamic diffusivity is increased, because diffusive processes become stronger relative to beach cusp growth owing to water particle diversion. For diffusivity $\gamma \geq 5$ m²/s, beach cusp formation is prevented and any preexisting features are smoothed (Figure 20b).

## 5. Discussion and Conclusions

[25] Field measurements of swash flow and morphology indicate that the height and cross-shore extent of beach cusps are tidally modulated. Beach cusps wane during rising tide owing to greater accretion in bays than on horns and a decrease in cross-shore extent. Beach cusps wax during falling tide owing to greater erosion in bays than on horns and an increase in cross-shore extent. These tidal modulations are hypothesized to originate with smoothing of morphology in the flow seaward of the swash front and with infiltration of swash during rising tide and exfiltration of groundwater during falling tide. A numerical model based on self-organization extended to include parameterizations of these two processes simulates qualitatively and, in some respects, quantitatively the observed formation and development of beach cusps, including tidal modulations in height and cross-shore extent. Simulations indicate that morphological smoothing is required to reproduce the observed cross-shore extent of the features and some aspects of their tidal modulations. The representation of smoothing in the model as diffusion, while accurately depicting redistribution of sediment in energetic conditions, does not explicitly treat the net erosion of sediment at horns and deposition at bays offshore of the swash zone [*Werner and Fink*, 1993; *Coco et al.*, 2000]. Overall, the role of infiltration in tidal modulation of beach cusps is minor, but it potentially can affect patterns in erosion and deposition

and changes in beach cusp height, especially on the upper beach.

[26] The model failed to predict details associated with reorientation and migration of beach cusps in all three experiments. In experiment A, this failure might be related partially to boundary effects, because of the relatively short stretch of beach measured. This failure also might originate with the lack of sea-surface gradient driven flow. During periods of obliquely incident waves, visual observations indicated swash often flowed over well-developed beach cusp horns. However, water particles in the model rarely climbed over horns, perhaps because the assumption that the sea surface is parallel to the beach is invalid for lateral swash flow on nonplanar morphology. In general, the model did not reproduce the magnitude nor the cross-shore pattern of erosion and deposition well, possibly because the model does not explicitly include the cross-shore balance between onshore transport owing to flow and transport asymmetries and offshore transport owing to gravity. The overprediction of the onshore extent of beach cusps in experiment B and to a lesser degree in experiment C might have originated with increased hydraulic conductivity caused by bulldozing of the natural beach, not accounted for in the model. Additionally, model predictions were degraded because of lack of measurements of swash flow during darkness. In summary, the model might be improved through treatment of the effects of sea-surface gradients on flow and better parameterization of cross-shore sediment transport seaward of the swash front. Nevertheless, the model reproduces many aspects of the observed tidal modulation of beach cusp development over a range of conditions using a single set of transport parameters.

## References

Antia, E. E. (1987), Preliminary field observations on beach cusp formation and characteristics on tidally and morphodynamically distinct beaches on the Nigerian coast, *Mar. Geol.*, *78*, 23–33.

Bear, J. (1972), *Dynamics of Fluids in Porous Media*, Elsevier Sci., New York.

Burnet, T. K. (1998), Field testing two beach cusp formation models, Ph.D. thesis, Duke Univ., Durham, N. C.

Butt, T., P. Russell, and I. Turner (2001), The influence of swash infiltration-exfiltration on beach face sediment transport: Onshore or offshore?, *Coastal Eng.*, *42*, 35–52.

Chafetz, H. S., and G. Kocurek (1981), Coarsening-upward sequences in beach cusp accumulations, *J. Sed. Petrol.*, *51*, 1157–1161.

Coco, G., T. J. O'Hare, and D. A. Huntley (1999), Beach cusps: A comparison of data and theories for their formation, *J. Coastal Res.*, *15*(3), 741–749.

Coco, G., D. A. Huntley, and T. J. O'Hare (2000), Investigation of a self-organisation model for beach cusp formation and development, *J. Geophys. Res.*, *105*(C9), 21,991–22,002.

Coco, D. A. Huntley, and T. J. O'Hare (2001), Regularity and randomness in the formation of beach cusps, *Mar. Geol.*, *178*, 1–9.

Coco, G., T. K. Burnet, B. T. Werner, and S. Elgar (2003), Test of self-organization in beach cusp formation, *J. Geophys. Res.*, *108*(C3), 3101, doi:10.1029/2002JC001496.

Dalrymple, R. A., and G. E. Lanan (1976), Beach cusp formed by intersecting waves, *Geol. Soc. Am. Bull.*, *87*, 57–60.

Dean, R. G., and E. M. Maurmeyer (1980), Beach cusps at Point Reyes and Drakes Bay Beaches, California, paper presented at 17th International Conference of Coastal Engineering, Am. Soc. of Civ. Eng., Reston, Va.

Dubois, R. N. (1978), Beach topography and beach cusps, *Geol. Soc. Am. Bull.*, *89*, 1133–1139.

Duncan, J. R. (1964), The effects of watertable and tide cycle on swash-backwash sediment distribution and beach profile development, *Mar. Geol.*, *2*, 186–197.

Eliot, I. G., and D. J. Clarke (1986), Minor storm impact on the beachface of a sheltered sandy beach, *Mar. Geol.*, *73*, 61–83.

Emery, K. O., and J. F. Foster (1948), Watertables in marine beaches, *J. Mar. Res.*, *7*, 644–654.

Evans, O. F. (1938), Classification and origin of beach cusps, *J. Geol.*, *46*, 615–627.

Falqués, A., A. Montoto, and V. Iranzo (1996), Bed-flow instability of the longshore current, *Cont. Shelf Res.*, *16*(5), 1927–1964.

Falqués, A., G. Coco, and D. A. Huntley (2000), A mechanism for the generation of wave-driven rhythmic patterns in the surf zone, *J. Geophys. Res.*, *105*(C10), 24,071–24,088.

Grant, U. S. (1948), Influence of the watertable on beach aggradation and degradation, *J. Mar. Res.*, *7*, 65–660.

Guza, R. T., and D. L. Inman (1975), Edge waves and beach cusps, *J. Geophys. Res.*, *80*(21), 2997–3012.

Inman, D. L., and R. T. Guza (1982), The origin of swash cusps on beaches, *Mar. Geol.*, *49*, 133–148.

Kuenen, P. H. (1948), The formation of beach cusps, *J. Geol.*, *97*, 34–40.

Longuet-Higgins, M. S., and D. W. Parkin (1962), Sea waves and beach cusps, *Geogr. J.*, *128*(2), 194–200.

Masselink, G. (1999), Alongshore variation in beach cusp morphology in a coastal embayment, *Earth Surf. Proc. Land.*, *24*, 335–348.

Masselink, G., and L. Li (2001), The role of swash infiltration in determining the beachface gradient: A numerical study, *Mar. Geol.*, *176*, 136–156.

Masselink, G., and C. B. Pattiaratchi (1998), Morphological evolution of beach cusp morphology and associated swash circulation patterns, *Mar. Geol.*, *146*, 93–113.

Masselink, G., B. J. Hegge, and C. B. Pattiaratchi (1997), Beach cusp morphodynamics, *Earth Surf. Proc. Land.*, *22*, 1139–1155.

McArdle, S. B., and A. McLachan (1991), Dynamics of the swash zone and effluent line on sandy beaches, *Mar. Ecol. Prog. Ser.*, *76*, 91–99.

Nielsen, P. (1990), Tidal dynamics of the water table in beaches, *Water Resour. Res.*, *26*(9), 2127–2134.

Russell, R. J., and W. G. McIntire (1965), Beach cusps, *Geol. Soc. Am. Bull.*, *76*, 307–320.

Schielen, R., A. Doelman, and H. E. de Swart (1993), On the nonlinear dynamics of free bars in straight channels, *J. Fluid Mech.*, *242*, 325–356.

Smith, D. D., and R. G. Dolan (1960), Erosional development of beach cusps along the outer banks of North Carolina, *Geol. Soc. Am. Bull*, 71, 1979 pp.

Takeda, I., and T. Sunamura (1983), Formation and spacing of beach cusps, *Coastal Eng. Jpn.*, *26*, 121–135.

Turner, I. L. (1995), Simulating the influence of groundwater seepage on sediment transported by the sweep of the swash zone across macro-tidal beaches, *Mar. Geol.*, *125*, 153–174.

Turner, I. L., and G. Masselink (1998), Swash infiltration-exfiltration and sediment transport, *J. Geophys. Res.*, *103*(C13), 30,813–30,824.

Werner, B. T., and T. M. Fink (1993), Beach cusps as self-organized patterns, *Science*, *260*, 968–971.

Williams, A. T. (1973), The problem of beach cusp development, *J. Sed. Petrol.*, *43*(3), 33–52.

—————————

T. K. Burnet and B. T. Werner, Complex Systems Laboratory, Cecil and Ida Green Institute of Geophysics and Planetary Physics, University of California, San Diego, La Jolla, CA 92093-0225, USA. (coco@ucsd.edu; bwerner@ucsd.edu)

G. Coco, National Institute of Water and Atmospheric Research, P.O. Box 11-115, Hamilton, New Zealand. (g.coco@niwa.co.nz)

S. Elgar, PVLAB, Woods Hole Oceanographic Institution, Woods Hole, MA 02543, USA. (elgar@whoi.edu)